Impaired upregulation of Stat2 gene restrictive to pancreatic β-cells is responsible for virus-induced diabetes in DBA-2 mice

三根, 敬一朗

Biochemical and Biophysical Research Communications 521 (2020) 853–860

Contents lists available at ScienceDirect

Biochemical and Biophysical Research Communications

journal homepage: www.elsevier.com/locate/ybbrc

Impaired upregulation of *Stat2* gene restrictive to pancreatic β-cells is responsible for virus-induced diabetes in DBA/2 mice

Keiichiro Mine [a, b, **, 1], Seiho Nagafuchi [b, *], Shinya Hatano [a], Kenichi Tanaka [b], Hitoe Mori [b], Hirokazu Takahashi [b], Keizo Anzai [b], Yasunobu Yoshikai [a]

[a] Division of Host Defense, Medical Institute of Bioregulation, Kyushu University, 3-1-1, Maidashi, Higashi-ku, Fukuoka, 812-8582, Japan
[b] Division of Metabolism and Endocrinology, Department of Internal Medicine, Faculty of Medicine, Saga University, 5-1-1, Nabeshima, Saga, 849-8501, Japan

ARTICLE INFO

Article history:
Received 18 October 2019
Accepted 29 October 2019
Available online 7 November 2019

Keywords:
Stat2
DBA/2
Virus-induced diabetes
β-Cell

ABSTRACT

Viral infection is a putative causal factor for the development of type 1 diabetes, but the exact pathogenic mechanism of virus-induced diabetes (VID) remains unclear. Here, to identify the critical factors that regulate VID, we analyzed encephalomyocarditis D (EMC-D) VID-sensitive DBA/2 mice in comparison with resistant B6 mice. EMC-D virus-induced cell death occurred more frequently in DBA/2 β-cells than in B6 β-cells with 100U/ml IFN-β priming *in vitro*. We therefore purified β-cells using flow cytometry from mice two days after EMC-D virus infection and subjected them to microarray analysis. As a results, innate immune response pathway was found to be enriched in B6 β-cells. The *signal transducer and activator of transcription 2* (*Stat2*) gene interacted with genes in the pathway. *Stat2* gene expression levels were lower in DBA/2 mice than in B6 mice, restrictive to β-cells. Moreover, administration of IFN-β failed to upregulate *Stat2* gene in DBA/2 β-cells than in those of B6 *in vivo*. The viral titer significantly increased only in the DBA/2 pancreas. Thus, these provided data suggest that impaired upregulation of *Stat2* gene restrictive to β-cells at the early stage of infection is responsible for VID development in DBA/2 mice.

1. Introduction

Type 1 diabetes (T1D) is caused by insulin-producing pancreatic β-cell destruction, usually leading to absolute insulin deficiency [1]. The number of T1D is increasing annually by approximately 3% [1,2]. Genetic factors have been widely reported as risk or protection factors for T1D; however, these risk factors cannot fully explain why the number of T1D cases has been increasing globally. The causal mechanisms for the increase in T1D prevalence remain unclear but may be due to changes in environmental risk factors and/or viral infections [2]. Human T1D research has suggested a close link with enterovirus, especially coxsackievirus B, which belongs to the *Picornaviridae* family. Enterovirus-associated VP1 antigen and enterovirus RNA are often detected in pancreatic islets, and an increase in anti-enterovirus antibodies has been observed in blood from T1D patients [3–5]. Furthermore, fulminant T1D, a clinical phenotype of T1D with abrupt onset, strongly suggests a viral contribution to the etiology [6].

In an experimental animal model, the D variant of EMC (EMC-D) virus, which belongs to the *Picornaviridae* family and harbors the capsid protein VP1 with Ala 152, induces diabetes in selected strains of inbred mice. After intraperitoneal infection with EMC-D virus, male SJL, SWR, and DBA/2 mice develop diabetes, while C57BL/6, AKR, and LP mice or female do not [7]. In contrast, the B variant of EMC virus, which possesses capsid protein VP1 with Thr152, does not induce diabetes in any strains of mice [8]. These observations demonstrate that the interplay between the genetic background of both the host and virus determines the outcome of VID [5,9]. This VID model is useful for analyzing the pathogenesis of VID and β-cell biology *in vivo* [10–12].

Viruses could contribute to diabetes development in several ways: direct β-cell virolysis, triggering β-cell-specific autoimmunity, bystander damage via local inflammation, and the induction of dedifferentiation [13,14]. Although innate immunity plays a central

* Corresponding author.
** Corresponding author. Division of Host Defense, Medical Institute of Bioregulation, Kyushu University, 3-1-1, Maidashi, Higashi-ku, Fukuoka, 812-8582, Japan.
E-mail addresses: k_mine@bioreg.kyushu-u.ac.jp (K. Mine), nagafu_s@med.kyushu-u.ac.jp (S. Nagafuchi).
[1] Research Fellow of Japan Society for the Promotion of Science.

https://doi.org/10.1016/j.bbrc.2019.10.193

role in protecting against picornavirus infection [15], the role of innate immune responses in VID is controversial [10,11,16–20]. In addition, the details of β-cell responses in viral infection associated conditions *in vivo* and the pathogenic mechanisms of VID are not fully understood. Here, we analyzed purified β-cells from EMC-D virus-infected mice and found that *Stat2* gene and antiviral genes expression was reduced specifically in DBA/2 β-cells at the early stage of infection; thus, impaired *Stat2* gene upregulation specific to β-cells is responsible for VID susceptibility in DBA/2 mice.

2. Materials and methods

2.1. Mice

C57BL/6 J, DBA/2 N, and B6D2F1 mice were purchased from Japan KBT. All mice were maintained under specific pathogen-free conditions and provided with food and water ad libitum. Age- and gender-matched mice were used for all experiments. This study was approved by the Committee of Ethics on Animal Experiments of the Faculty of Medicine, Kyushu University (A30-128-0), and Faculty of Medicine, Saga University (29-045-0). Experiments were carried out according to local guidelines for animal experimentation. Blood glucose levels were measured using the glucose oxidase method (Sanwa kagaku kenkyusho). Levels of IFNs were measured by ELISA (pbl Assay Science).

2.2. Virus

EMC-D virus was kindly provided by Dr. A.L. Notokins, NIH, USA, and J-W Yoon, University of Calgary, Canada.

2.3. Histopathology

Pancreas specimens were immersed in 4% (w/v) paraformaldehyde overnight at 4 °C and then embedded in paraffin. Cut sections (4 μm) were subjected to hematoxylin and eosin (H&E) or immunofluorescence staining. See supplemental material for detailed information.

2.4. Quantitative PCR

Total RNA from MEFs was extracted using ISOGENII (Nippon Gene), and total RNA from pancreatic β-cells was extracted using NucleoSpin RNA XS (Mna). The RNA quality was verified by running samples on an Agilent 2100 Bioanalyzer (Agilent Technologies). cDNA was synthesized using a High Capacity cDNA Reverse Transcription Kit (Applied Biosystems) and analyzed using PowerUP SYBR Green Master Mix (Applied Biosystems) and an ABI 7500 Real-Time PCR System (Applied Biosystems). All gene expression values were relative to the Gapdh signal. See Table S2 for primers used.

2.5. Islet isolation, mouse embryonic fibroblast (MEF) preparation and cell death assay

Islets were isolated using 1 mg/ml collagenase-P (Roche) and Histopaque-1077 (Sigma Aldrich) as previously described [21] with minor modifications. β-cells were stained with an Apoptotic/Necrotic Cell Detection Kit (PromoKine). MEFs were prepared from C57BL/6 or DBA/2 E13 to E14 embryos. See supplemental material for detailed information.

2.6. Purification of pancreatic β-cells using flow cytometry

Purification of β-cells was performed as previously described [22]. Briefly, islets were dissociated using TrypLE express for 9 min at 37 °C. Dissociated islet cells were washed with RPMI1640 containing 10% FBS and resuspended in medium. Dissociated islet cells were stained with FluoZin-3-AM (Invitrogen) and tetramethylrhodamine ethyl ester perchlorate (TMRE; Life Technologies) and an anti-Cd45 antibody (BD) for 30 min at 37 °C. FluoZin-3-AM-positive and TMRE-positive cells were sorted using a FACSAria II (BD) (Fig. S3A). We added 1 mg/mL propidium iodide (Sigma Aldrich) to the cell suspension just before flow cytometry.

2.7. Microarray analysis

We used an Affymetrix Clariom D Assay Mouse Array for the analysis. Microarray analysis was kindly provided by Cell Innovator (Fukuoka, Japan). The accession number for the data is GEO: GSE132388.

2.8. siRNA

Cells were transiently transfected with siRNA or control siRNA using Opti-MEM (Gibco) and Lipofectamine 3000 reagent (Invitrogen). After 24 h of incubation with the transfection reagent, the medium was changed, and mouse IFN-β (100 U/ml) was added. After 3 h of stimulation with IFN-β, total RNA was extracted using ISOGENII. See Table S3 for siRNAs used.

2.9. Statistical analysis

Statistical analysis was performed using the statistical program R (http://cran.r-project.org). Values of $p < 0.05$ were considered to represent statistically significant differences. All data are expressed as the mean ± sem. $^{*}p < 0.05$, $^{**}p < 0.01$; two-sample *t*-test.

3. Results

3.1. Administration of type 1 IFNs failed to overcome the VID

To assess the clinical course of EMC-D VID, we intraperitoneally challenged male B6 and DBA/2 mice with 1×10^3 PFU of EMC-D virus. The viral titer was significantly increased in the DBA/2 pancreas three days after infection (Fig. 1A). Effective viral clearance at five to seven days post infection was observed in both the B6 and DBA/2 pancreas (Fig. 1A), suggesting that viral growth levels within three days after infection are critically associated with the development of diabetes. Levels of serum type 1 IFNs concentration and gene expression of type 1 IFNs in MEFs after EMC-D virus infection were variable but tend to be higher in DBA/2 mice (Fig. 1B,S1). To ascertain the role of type 1 IFNs precisely *in vivo*, we performed adoptive transfer of type 1 IFNs after infection for four consecutive days, and found that even high-dose type 1 IFNs could not prevent EMC-D VID in DBA/2 mice (Fig. 1C). DBA/2 islets with or without type 1 IFN transfer were extensively damaged and had a markedly decreased number of insulin-positive cells (Fig. 1D and E). These results raised the possibility that candidate molecules responsible for VID involved downstream of the type 1 IFN signaling pathway but not the type 1 IFN production pathway.

To clarify the genetic basis of susceptibility to EMC-D VID, F1 hybrid mice (B6D2F1 and D2B6F1) were also infected with EMC-D virus. Male F1 hybrid mice developed EMC-D VID (Fig. 1F), indicating that the molecule controlling susceptibility to EMC-D VID operates in a dominant fashion.

3.2. DBA/2 islets are damaged before immune cell infiltration

We found that both B6 and DBA/2 islets had mild infiltration of

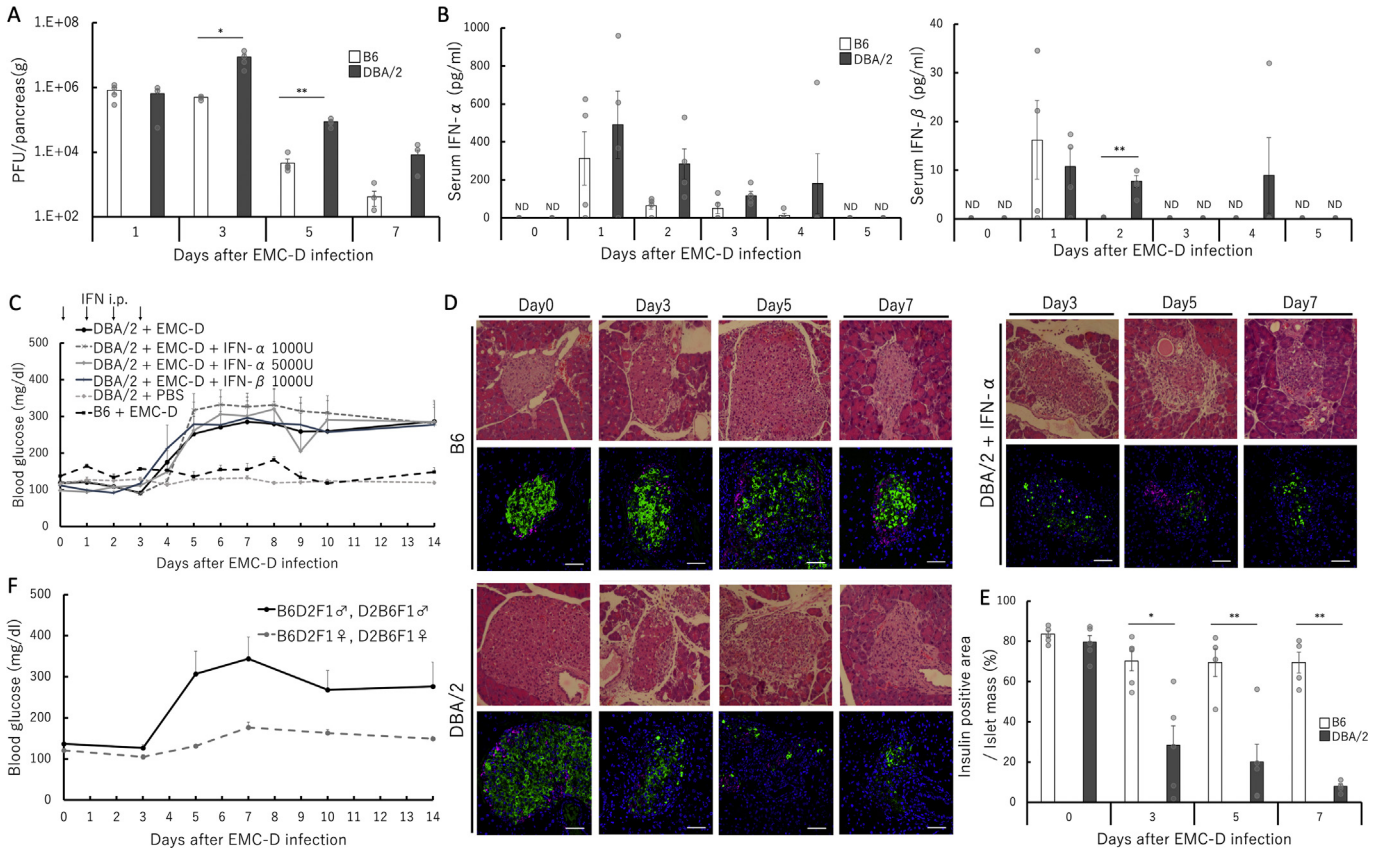

Fig. 1. Ineffectiveness of IFN to resist against EMC-D VID. **(A)** Viral titers in the pancreas (n = 3–4). **(B)** Serum IFN-α and IFN-β concentrations (n = 4). **(C)** Blood glucose levels (n = 4–9). Animals with blood glucose levels exceeding 250 mg/dl were diagnosed as diabetic. **(D)** Histopathology of paraffin-embedded pancreas sections stained with H&E or anti-insulin (green) and anti-glucagon (magenta). Scale bar, 50 μm. **(E)** Insulin positive areas in the islet cell mass (n = 4–5). **(F)** Blood glucose levels in B6xDBA/2 F1 mice (n = 7).

Cd45-positive cells at three days after infection, while insulin-negative areas, possibly damaged β-cells, were observed only in DBA/2 islets (Fig. 2A). At five days after infection, in contrast to B6 mice, DBA/2 mice showed severe Cd45-positive cell infiltration into the islets along with extensive islet destruction (Fig. 2A). These observations suggest that virus-induced islet-cell lysis, coinciding with peak of viral replication in the pancreas (Fig. 1A), is the first step of islet-cell destruction followed by inflammatory cell infiltration into the islets.

3.3. DBA/2 β-cells show reduced responsiveness to type 1 IFN

To clarify whether target-cell defense is important to prevent VID, we assessed virus-induced β-cell death *in vitro*. Isolated islets were cultured with or without IFN-β, and infected with EMC-D virus. IFN-β per se did not induce β-cell death under the tested condition (Figs. S2A and B). Following EMC-D infection, IFN-β priming (100 U/ml) increased the staining of healthy nuclei in B6 β-cells but not in DBA/2 β-cells (Fig. 2B and C). Annexin V staining, a marker of apoptosis, was increased in DBA/2 β-cells (Fig. 2B and C). However, MEFs showed comparable healthy nuclear staining under the same condition (Fig. 2D and E). In contrast to *in vivo* IFN administration (Fig. 1C), a high dose of IFN-β priming maintained DBA/2 β-cell health *in vitro* (Figs. S2C and D), suggesting that both virus-mediated direct cell lysis and immune cell-mediated inflammation induce β-cell damage *in vivo*. The number of cells positive for Caspase-3, another apoptosis marker, was increased only in DBA/2 islets *in situ* at day five (Fig. S2G). These observations taken together suggest that β-cell death is caused by virolysis at the early stage of infection, and β-cell death is apparently enhanced by local inflammation, which may induce apoptosis, occurring throughout the clinical course. Thus, these findings suggest that DBA/2 β-cells are damaged by EMC-D virus due to impaired cell type-specific responsiveness to type 1 IFN.

3.4. Innate immune response pathway is enriched in B6 β-cells

To assess the context-specific gene expression profile in β-cells, viable β-cells were stained with FluoZin-3-AM and TMRE [22], purified by flow cytometry from two days after EMC-D infected mice (Fig. S3A), and devoted to microarray analysis. We found that 290 out of 26596 gene probes were expressed significantly higher in B6 β-cells than DBA/2 β-cells (>twofold, $p < 0.05$) (Fig. 3A). The 114 of the 290 highly expressed gene probes in B6 β-cells were ISGs induced by type 1 and 2 IFNs (Fig. S3B). The gene ontology (GO) biological process enrichment analysis showed that differentially expressed genes in B6 β-cells were most enriched in the innate immune response pathway ($p < 4.5E-20$) (Fig. 3B). Moreover, we conducted a microarray analysis for B6D2F1 β-cells derived from two days after infected B6D2F1 mice (Fig. 3C). Differentially expressed 702 genes in B6 β-cells also showed enrichment for the innate immune response pathway ($p < 3.8E-33$) (Fig. 3D). Virus recognition molecules and IFN associated genes tended to be highly expressed in B6 β-cells than in DBA/2 and B6D2F1 β-cells (Fig. S3C). In contrast, differentially expressed genes in DBA/2 and B6D2F1 β-cells did not show enrichment of immune-related pathways (Fig. 3B,D). The microarray data revealed that apoptosis-related genes were not upregulated in DBA/2 β-cells at two days after

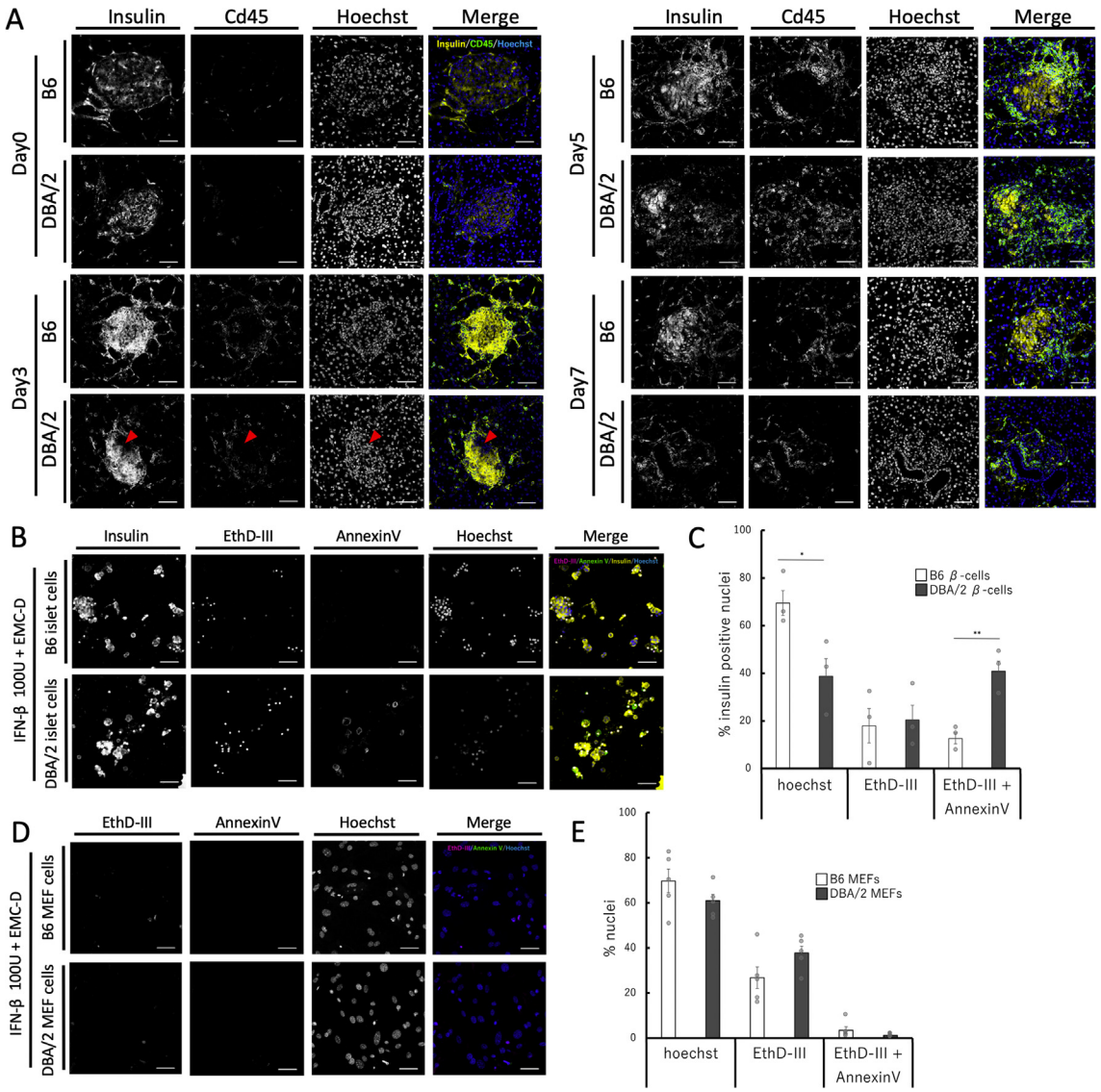

Fig. 2. Reduced responsiveness to type 1 IFNs in DBA/2 β-cells. **(A)** Confocal images of frozen sections of pancreas stained as indicated. Red arrows indicate the damaged area. **(B)** Confocal images of isolated B6 or DBA/2 β-cells, following 100 U/ml IFN-β treatment; stained as indicated. **(C)** The percentage of EthD-III, Annexin-V-positive cells among insulin-positive cells (n = 3). **(D)** Confocal images of MEFs followed by 100 U/ml IFN-β treatment; stained as indicated. **(E)** The percentage of EthD-III, Annexin-V-positive cells among MEFs (n = 5). Scale bar, 50 μm.

infection. All chemokines were expressed at higher or comparable levels in B6 β-cells, except for *Cxcl11*, *Ccl25*, and *Cx3cl1*. There were only a few signatures of endoplasmic reticulum (ER) stress and β-cell dedifferentiation in DBA/2 β-cells (Fig. S3C). Comparable expression levels were observed in IFN receptors. Notably, the expression of many antiviral genes was impaired in DBA/2 and B6D2F1 β-cells than in B6 β-cells (Fig. 3E). These *in vivo* viral infection associated condition-specific transcriptomic analyses suggest that, at the early stage of infection, the innate immune responses are impaired in DBA/2 and B6D2F1 β-cells.

3.5. Identification of hub gene, orchestrating innate immune responses in β-cells

To identify important gene associated with VID, we analyzed 158 gene probes that overlap among the genes differentially expressed between B6 β-cells and DBA/2 β-cells or B6D2F1 β-cells (Fig. 4A). These overlapping gene probes also showed enrichment of the innate immune response pathway ($p < 3.9E-15$) (Fig. 4B). Because intact innate immune responses are critical to prevent EMC-D VID [10,11,17], we analyzed the 19 genes contained in the pathway. We first examined the genetic variations of these 19 genes, and found that 9 genes (*Oas2*, *Krt16*, *Acord1*, *Ighg2b*, *H2-q7*, *Gbp4*, *Cfb*, *C3*, and *C1ra*) did not have any SNPs, indels or structural variants within the proximal promoter region (−300 to +50 bp from the transcription start site; Fig. 4C). Given that mutations within the proximal promoter region were not found in the all genes (Fig. 4C), and a broad range of antiviral genes were expressed at lower levels in DBA/2 and B6D2F1 β-cells (Fig. 3E), the gene that interacts with a broad range of antiviral genes may orchestrate the gene expression profile. We therefore explored hub gene interactions with the 19 genes and found that the *Stat2* gene interacted with 10 out of the 19 genes (Fig. 4D). *Stat2* gene expression was reduced by approximately 40% in DBA/2 β-cells and 70% in B6D2F1 β-cells compared with that in B6 β-cells (Fig. 3E). Since Stat2 is a key transcription factor leading to the activation of ISGs

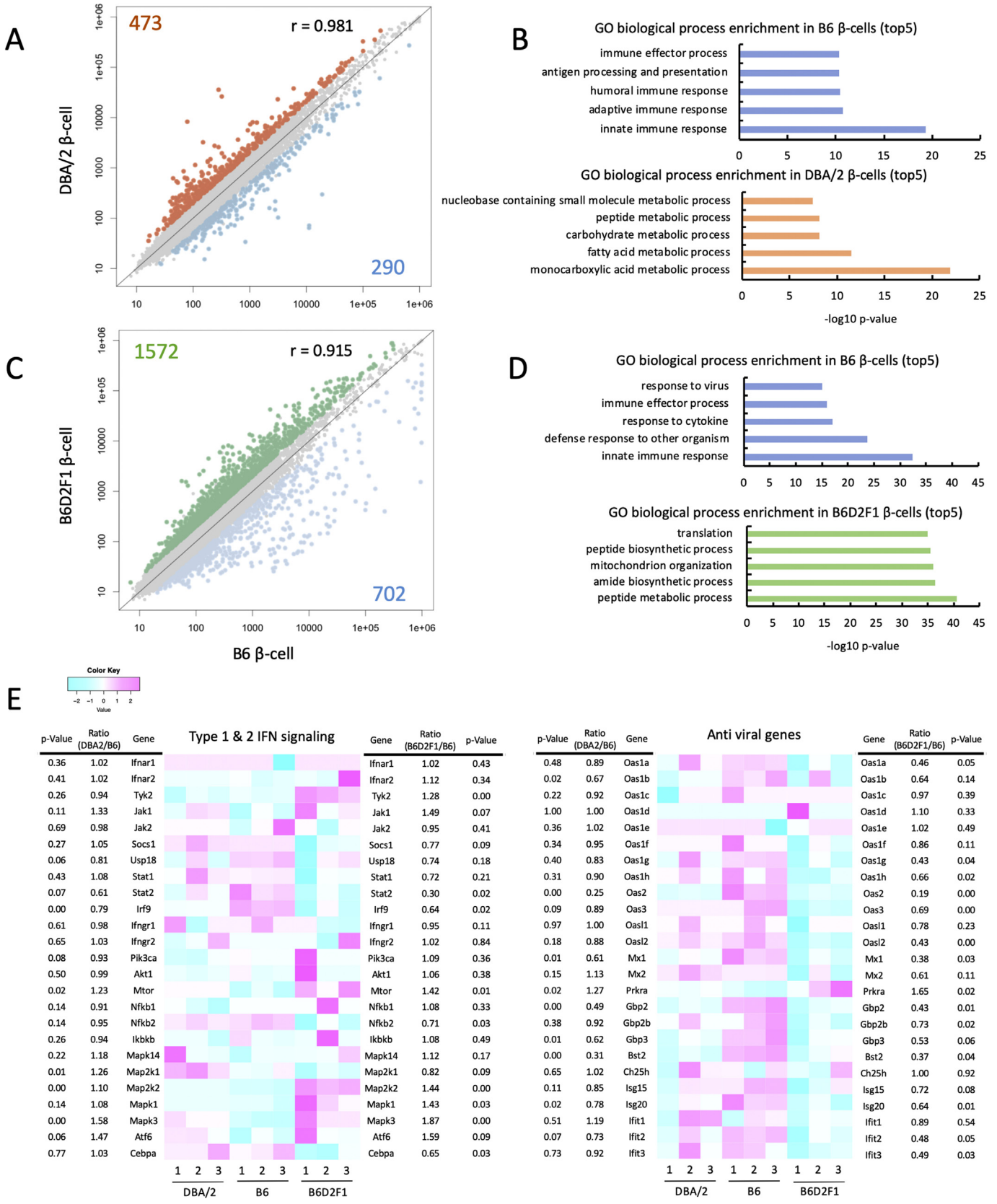

p-Value	Ratio (DBA2/B6)	Gene	Gene	Ratio (B6D2F1/B6)	p-Value
0.36	1.02	Ifnar1	Ifnar1	1.02	0.43
0.41	1.02	Ifnar2	Ifnar2	1.12	0.34
0.26	0.94	Tyk2	Tyk2	1.28	0.00
0.11	1.33	Jak1	Jak1	1.49	0.07
0.69	0.98	Jak2	Jak2	0.95	0.41
0.27	1.05	Socs1	Socs1	0.77	0.09
0.06	0.81	Usp18	Usp18	0.74	0.18
0.43	1.08	Stat1	Stat1	0.72	0.21
0.07	0.61	Stat2	Stat2	0.30	0.02
0.00	0.79	Irf9	Irf9	0.64	0.02
0.61	0.98	Ifngr1	Ifngr1	0.95	0.11
0.65	1.03	Ifngr2	Ifngr2	1.02	0.84
0.08	0.93	Pik3ca	Pik3ca	1.09	0.36
0.50	0.99	Akt1	Akt1	1.06	0.38
0.02	1.23	Mtor	Mtor	1.42	0.01
0.14	0.91	Nfkb1	Nfkb1	1.08	0.33
0.14	0.95	Nfkb2	Nfkb2	0.71	0.03
0.26	0.94	Ikbkb	Ikbkb	1.08	0.49
0.22	1.18	Mapk14	Mapk14	1.12	0.17
0.01	1.26	Map2k1	Map2k1	0.82	0.09
0.00	1.10	Map2k2	Map2k2	1.44	0.00
0.14	1.08	Mapk1	Mapk1	1.43	0.03
0.00	1.58	Mapk3	Mapk3	1.87	0.00
0.06	1.47	Atf6	Atf6	1.59	0.09
0.77	1.03	Cebpa	Cebpa	0.65	0.03

p-Value	Ratio (DBA2/B6)	Gene	Gene	Ratio (B6D2F1/B6)	p-Value
0.48	0.89	Oas1a	Oas1a	0.46	0.05
0.02	0.67	Oas1b	Oas1b	0.64	0.14
0.22	0.92	Oas1c	Oas1c	0.97	0.39
1.00	1.00	Oas1d	Oas1d	1.10	0.33
0.36	1.02	Oas1e	Oas1e	1.02	0.49
0.34	0.95	Oas1f	Oas1f	0.86	0.11
0.40	0.83	Oas1g	Oas1g	0.43	0.04
0.31	0.90	Oas1h	Oas1h	0.66	0.02
0.00	0.25	Oas2	Oas2	0.19	0.00
0.09	0.89	Oas3	Oas3	0.69	0.00
0.97	1.00	Oasl1	Oasl1	0.78	0.23
0.18	0.88	Oasl2	Oasl2	0.43	0.00
0.01	0.61	Mx1	Mx1	0.38	0.03
0.15	1.13	Mx2	Mx2	0.61	0.11
0.02	1.27	Prkra	Prkra	1.65	0.02
0.00	0.49	Gbp2	Gbp2	0.43	0.01
0.38	0.92	Gbp2b	Gbp2b	0.73	0.02
0.01	0.62	Gbp3	Gbp3	0.53	0.06
0.00	0.31	Bst2	Bst2	0.37	0.04
0.65	1.02	Ch25h	Ch25h	1.00	0.92
0.11	0.85	Isg15	Isg15	0.72	0.08
0.02	0.78	Isg20	Isg20	0.64	0.01
0.51	1.19	Ifit1	Ifit1	0.89	0.54
0.07	0.73	Ifit2	Ifit2	0.48	0.05
0.73	0.92	Ifit3	Ifit3	0.49	0.03

Fig. 3. Innate immune responses are enriched in B6 β-cells. **(A)** Transcriptional profiling of β-cells. Blue dots and numbers indicate transcripts increased in B6 β-cells; orange dots and numbers indicate transcripts increased in DBA/2 β-cells. **(B)** Top 5 GO biological process pathways. **(C)** Transcriptional profiling of β-cells. Blue dots and numbers indicate transcripts increased in B6 β-cells; green dots and numbers indicate transcripts increased in B6D2F1 β-cells. **(D)** Top 5 GO biological process pathways. **(E)** Heatmap showing the transcripts of selected genes.

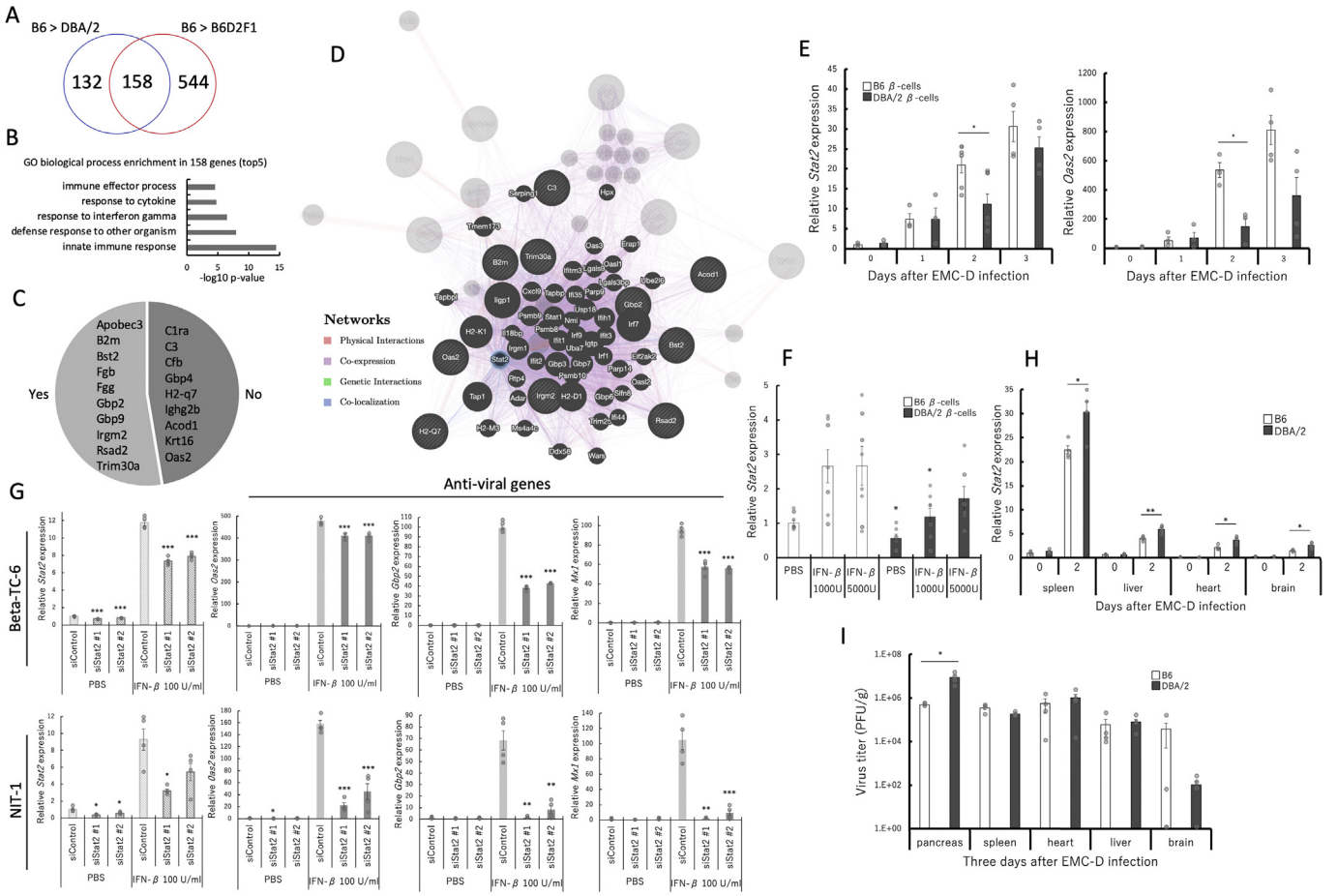

Fig. 4. Impaired upregulation of *Stat2* gene in DBA/2 β-cells. **(A)** The overlapping genes differentially expressed between B6 and DBA/2 or B6D2F1 β-cells. **(B)** Top 5 GO biological process pathways. **(C)** Genes harbored in DBA/2 mice with (yes) or without (no) mutations within the proximal promoter region. **(D)** Gene network analysis. Genes interacting with the *Stat2* gene are highlighted. **(E)** qPCR of the *Stat2* and *Oas2* genes expression in β-cells (n = 3–5). **(F)** qPCR of the *Stat2* gene post IFN-β administration (n = 6–8). **(G)** qPCR of the *Stat2*, *Oas2*, *Gbp 2*, and *Mx1* gene expressions (n = 4) following *Stat2* gene knocked down. **(H)** qPCR of the *Stat2* gene expression in organs (n = 4). **(I)** Viral titers in the indicated organs. The data of pancreas are quoted from Fig. 1A.

[23], we focused on *Stat2* gene expression conditions.

3.6. Upregulation of Stat2 gene is impaired in DBA/2 β-cells

qPCR confirmed the low *Stat2* gene expression level with statistical significance in DBA/2 β-cells at two days post infection (Fig. 4E); however, *Stat2* gene expression at one day post infection was comparable. Antiviral *Oas2* gene expression levels were also lower in DBA/2 β-cells at two days after infection (Fig. 4E). Moreover, IFN-β administration failed to upregulate *Stat2* gene in DBA/2 β-cells than in B6 β-cells (Fig. 4F). To evaluate the reduced *Stat2* gene expression in β-cells, siRNAs targeting the *Stat2* gene, were transiently transfected into β-cell lines. The approximately 40% reduction of *Stat2* gene expression in response to IFN-β mimicked that of the EMC-D viral infection condition in DBA/2 β-cells at day two. *Stat2* gene knockdown caused a dramatic reduction of ISGs expression in β-cells (Fig. 4G), suggesting that impaired upregulation of *Stat2* gene lead to reduced antiviral responses in DBA/2 β-cells.

Interestingly, *Stat2* gene expression in organs other than β-cells at two days after infection was significantly higher in DBA/2 mice than in B6 mice (Fig. 4H). Antiviral genes were expressed at comparable or higher levels in DBA/2 organs than in B6 organs, except for *Oas2* in splenic cells (Fig. S4A). Consistent with these findings, significantly high viral titers were observed in the pancreas but not in other organs (Fig. 4I). In the *Stat2* gene locus, no SNPs, indels or structural variants were detected in the DBA/2 genome sequence. In addition, the methylation status of the CpG site in the *Stat2* gene at two days after infection was comparable (Fig. S4B). These data suggest that *Stat2* gene expression levels in β-cells may be upregulated by unknown factor specific to β-cells.

4. Discussion

Here, we found impaired upregulation of *Stat2* gene solely in β-cells and an impaired innate immune response in DBA/2 β-cells under challenged condition by diabetogenic virus *in vivo*. Consistent with our data, the importance of innate immunity against β-cell-tropic viruses has been reported [10,11,17]. Intriguingly, although *Stat2* gene expression levels were comparable between DBA/2 and B6 mice before infection in any organs, at two days after infection, the levels were significantly reduced specific to DBA/2 β-cells (Fig. 4E,H). Our results suggest that impaired upregulation of important genes at cell type-specific and condition-specific may be one of the causes of disease progression. It is suggests that *Stat2* gene expression in β-cells is regulated by cell type-specific and viral infection condition-associated regulatory mechanisms. Accordingly, stimulation-responsive immune enhancers have recently been studied [24,25]. SNPs located in a context-specific enhancer did not entirely block target gene expression but rather delayed the

timing of gene upregulation in response to extracellular stimuli [25]. Given that DBA/2 mice have the same *Stat2* genome sequence and methylation status as B6 mice, SNPs harbored by DBA/2 mice may possibly disrupt the β-cell-specific stimulation-responsive immune enhancer for the *Stat2* gene, leading to a delay in the gene upregulation. Identification of responsible SNPs for the regulation of *Stat2* expression is required.

Based on the gene interaction analysis (Fig. 4D), in the 19 genes involved in the innate immune response pathway, we found *Stat2* is not interacted with 9 genes (*Apobec3*, *C1ra*, *Cfb*, *Fgb*, *Fgg*, *Gbp4*, *Ighg2b*, *Krt16*, and *Gbp9*). The data indicate that other gene(s) except for *Stat2* also associated with the innate immune responses and the phenotype of DBA/2 β-cells. The microarray data revealed that not only type 1 but also type 2 IFN regulated gene expression levels were upregulated in β-cells (Fig. S3B). Antiviral genes such as Gbp4 and Gbp9 which are not regulated by Stat2 (Fig. 4D) are induced by type 1 IFNs or IFN-γ, implying that IFN-γ might contribute to resist against EMC-D VID.

The present study suggests that impaired upregulation of condition-dependent *Stat2* gene restrictive to β-cells is critical for progression of EMC-D VID in DBA/2 mice. Intriguingly, the human genome 12q13.2 locus, including the *STAT2* gene, is associated with T1D [26]. The identification of the key genomic region that control *Stat2* gene expression in β-cells will contribute to clarifying the pathogenesis of diabetes in mice and humans. The organ-specific regulatory mechanisms of gene expression have not been fully documented, requiring further studies. This animal model will also contribute to clarify the organ-specific regulation of target genes.

Declaration of competing interest

The authors have no potential conflict of interest relevant to this article to report.

Acknowledgments

The authors are grateful to N. Noguchi, H. Yamada, T. Murakami, X. Tun, and D. Yue for giving counsel about experiments, and Y. Kitada, A. Yano, and C. Ogawa for helping to prepare the manuscript, and K. Ichikawa for helping the histopathology experiments. We appreciate the technical support by the Research Support Center, Graduate School of Medical Sciences, Kyushu University; Laboratory for Technical Support, Medical Institute of Bioregulation, Kyushu University; and Analytical Research Center for Experimental Sciences, Saga University. This work was supported by a Grant-in-Aid for JSPS Fellows [17J03060], a Grant-in-Aid for Scientific Research B [18H02853], and a Japan IDDM Network Research Grant.

Appendix A. Supplementary data

Supplementary data to this article can be found online at https://doi.org/10.1016/j.bbrc.2019.10.193.

Conflicts of interest

None.

References

[1] American Diabetes association, Diagnosis and classification of diabetes mellitus, Diabetes Care 27 (2004) S5–S10, https://doi.org/10.1016/j.autrev.2014.01.020.
[2] International Diabetes Federation, Eighth edition, , 2017, 2017.
[3] F. Dotta, S. Censini, A.G.S. van Halteren, L. Marselli, M. Masini, S. Dionisi, F. Mosca, U. Boggi, A.O. Muda, S. Del Prato, J.F. Elliott, A. Covacci, R. Rappuoli, B.O. Roep, P. Marchetti, Coxsackie B4 virus infection of beta cells and natural killer cell insulitis in recent-onset type 1 diabetic patients, Proc. Natl. Acad. Sci. 104 (2007) 5115–5120, https://doi.org/10.1073/pnas.0700442104.
[4] S. Tanaka, Y. Nishida, K. Aida, T. Maruyama, A. Shimada, M. Suzuki, H. Shimura, S. Takizawa, M. Takahashi, D. Akiyama, S. Arai-yamashita, F. Furuya, A. Kawaguchi, M. Kaneshige, R. Katoh, T. Endo, Enterovirus infection, CXC chemokine ligand 10 (CXCL10), and CXCR3 circuit a mechanism of accelerated β-cell failure in fulminant type 1 diabetes, Diabetes 58 (2009) 2285–2291, https://doi.org/10.2337/db09-0091.S.Tan.
[5] D. Hober, P. Sauter, Pathogenesis of type 1 diabetes mellitus: interplay between enterovirus and host, Nat. Rev. Endocrinol. 6 (2010) 279–289, https://doi.org/10.1038/nrendo.2010.27.
[6] A. Imagawa, T. Hanafusa, Fulminant type 1 diabetes-an important subtype in East Asia, Diabetes. Metab. Res. Rev. 27 (2011) 959–964, https://doi.org/10.1002/dmrr.1236.
[7] J.W. Yoon, P.R. McClintock, T. Onodera, A.L. Notkins, Virus-induced diabetes mellitus. XVIII. Inhibition by a nondiabetogenic variant of encephalomyocarditis virus, J. Exp. Med. 152 (1980) 878–892. http://www.ncbi.nlm.nih.gov/pubmed/6252275%0A. http://www.pubmedcentral.nih.gov/articlerender.fcgi?artid=PMC2185964.
[8] H.S. Jun, Y. Kang, H.S. Yoon, K.H. Kim, A.L. Notions, J.W. Yoon, Determination of encephalomyocarditis vital diabetogenicity by a putative binding site of the viral capsid protein, Diabetes 47 (1998) 576–582, https://doi.org/10.2337/diabetes.47.4.576.
[9] S. Nagafuchi, A. Toniolo, Viral diabetes: virus diabetogenicity and host susceptibility, Immunoendocrinology 2 (2015) 1–13, https://doi.org/10.14800/ie.1026.
[10] K. Izumi, K. Mine, Y. Inoue, M. Teshima, S. Ogawa, Y. Kai, T. Kurafuji, K. Hirakawa, D. Miyakawa, H. Ikeda, A. Inada, M. Hara, H. Yamada, K. Akashi, Y. Niho, K. Ina, T. Kobayashi, Y. Yoshikai, K. Anzai, T. Yamashita, H. Minagawa, S. Fujimoto, H. Kurisaki, K. Shimoda, H. Katsuta, S. Nagafuchi, Reduced Tyk2 gene expression in β-cells due to natural mutation determines susceptibility to virus-induced diabetes, Nat. Commun. 6 (2015) 6748, https://doi.org/10.1038/ncomms7748.
[11] S.A. Mccartney, W. Vermi, S. Lonardi, C. Rossini, K. Otero, B. Calderon, S. Gilfillan, M.S. Diamond, E.R. Unanue, M. Colonna, RNA sensor – induced type I IFN prevents diabetes caused by a β cell – tropic virus in mice, J. Clin. Investig. 121 (2011) 1497–1507, https://doi.org/10.1172/JCI44005.es.
[12] K. Aida, T. Kobayashi, A. Takeshita, E. Jimbo, Y. Nishida, S. Yagihashi, M. Hosoi, T. Fukui, A. Sugawara, S. Takasawa, Crucial role of Reg I from acinar-like cell cluster touching with islets (ATLANTIS) on mitogenesis of beta cells in EMC virus-induced diabetic mice, Biochem. Biophys. Res. Commun. 503 (2018) 963–969, https://doi.org/10.1016/j.bbrc.2018.06.103.
[13] A. Op De Beeck, D.L. Eizirik, Viral infections in type 1 diabetes mellitus — why the β cells ? Nat. Publ. Gr. 12 (2016) 263–273, https://doi.org/10.1038/nrendo.2016.30.
[14] M. Oshima, K.-P. Knoch, M. Diedisheim, A. Petzold, P. Cattan, M. Bugliani, P. Marchetti, P. Choudhary, G.-C. Huang, S.R. Bornstein, M. Solimena, O. Albagli-Curiel, R. Scharfmann, Virus-like infection induces human β cell dedifferentiation, JCI Insight 3 (2018), https://doi.org/10.1172/jci.insight.97732.
[15] O. Takeuch, S. Akira, Innate immunity to virus infection, Immunol. Rev. 227 (2009) 75–86, https://doi.org/10.1111/j.1600-065X.2008.00737.x.
[16] L. Marroqui, R.S. Dos Santos, T. Fløyel, F.A. Grieco, I. Santin, A. Op De Beeck, L. Marselli, P. Marchetti, F. Pociot, D.L. Eizirik, TYK2, a candidate gene for type 1 diabetes, modulates apoptosis and the innate immune response in human pancreatic β-cells, Diabetes 64 (2015) 3808–3817, https://doi.org/10.2337/db15-0362.
[17] M. Flodström, A. Maday, D. Balakrishna, M.M. Cleary, A. Yoshimura, N. Sarvetnick, Target cell defense prevents the development of diabetes after viral infection, Nat. Immunol. 3 (2002) 373–382, https://doi.org/10.1038/ni771.
[18] Y. Hosokawa, T. Toyoda, K. Fukui, M.Y. Baden, M. Funato, Y. Kondo, T. Sudo, H. Iwahashi, M. Kishida, C. Okada, A. Watanabe, I. Asaka, K. Osafune, A. Imagawa, I. Shimomura, Insulin-producing Cells Derived from 'induced Pluripotent Stem Cells' of Patients with Fulminant Type 1 Diabetes: Vulnerability to Cytokine Insults and Increased Expression of Apoptosis-Related Genes, 2018, https://doi.org/10.1111/jdi.12727.
[19] S. Nagafuchi, Y. Kamada-Hibio, K. Hirakawa, N. Tsutsu, M. Minami, A. Okada, K. Kai, M. Teshima, A. Moroishi, Y. Murakami, Y. Umeno, Y. Yokogawa, K. Kogawa, K. Izumi, K. Anzai, R. Iwakiri, K. Hamaguchi, N. Sasaki, S. Nohara, E. Yoshida, M. Harada, K. Akashi, T. Yanase, J. Ono, T. Okeda, R. Fujimoto, K. Ihara, T. Hara, Y. Kikuchi, M. Iwase, T. Kitazono, F. Kojima, S. Kono, H. Kurisaki, S. Kondo, H. Katsuta, TYK2 promoter variant and diabetes mellitus in the Japanese, EBioMedicine 2 (2015) 744–749, https://doi.org/10.1016/j.ebiom.2015.05.004.
[20] K. Mine, K. Hirakawa, S. Kondo, M. Minami, A. Okada, N. Tsutsu, Y. Yokogawa, Y. Hibio, F. Kojima, S. Fujimoto, H. Kurisaki, K. Anzai, Y. Yoshikai, S. Nagafuchi, Subtyping of type 1 diabetes as classified by anti-GAD antibody, IgE levels, and tyrosine kinase 2 (TYK2) promoter variant in the Japanese, EBioMedicine 23 (2017) 46–51, https://doi.org/10.1016/j.ebiom.2017.08.012.
[21] E.J. Zmuda, C.A. Powell, T. Hai, A method for murine islet isolation and subcapsular kidney transplantation, J. Vis. Exp. (2011) 1–11, https://doi.org/10.3791/2096.
[22] S. Jayaraman, Assessment of beta cell viability, Curr. Protoc. Cytom. 55 (2011)

6.27.1–6.27.16, https://doi.org/10.1097/NUR.0000000000000066.
[23] H.C. Steen, A.M. Gamero, STAT2 phosphorylation and signaling, JAK-STAT 2 (2013), https://doi.org/10.4161/jkst.25790 e25790.
[24] K. Alasoo, J. Rodrigues, S. Mukhopadhyay, A.J. Knights, A.L. Mann, K. Kundu, C. Hale, G. Dougan, D.J. Gaffney, Shared genetic effects on chromatin and gene expression indicate a role for enhancer priming in immune response, Nat. Genet. 50 (2018) 424–431, https://doi.org/10.1038/s41588-018-0046-7.
[25] D.R. Simeonov, B.G. Gowen, M. Boontanrart, T.L. Roth, J.D. Gagnon, M.R. Mumbach, A.T. Satpathy, Y. Lee, N.L. Bray, A.Y. Chan, D.S. Lituiev, M.L. Nguyen, R.E. Gate, M. Subramaniam, Z. Li, J.M. Woo, T. Mitros, G.J. Ray, G.L. Curie, N. Naddaf, J.S. Chu, H. Ma, E. Boyer, F. Van Gool, H. Huang, R. Liu, V.R. Tobin, K. Schumann, M.J. Daly, K.K. Farh, K.M. Ansel, C.J. Ye, W.J. Greenleaf, M.S. Anderson, J.A. Bluestone, H.Y. Chang, J.E. Corn, A. Marson, Discovery of stimulation-responsive immune enhancers with CRISPR activation, Nature 549 (2017) 111–115, https://doi.org/10.1038/nature23875.
[26] J.P. Bradfield, H.Q. Qu, K. Wang, H. Zhang, P.M. Sleiman, C.E. Kim, F.D. Mentch, H. Qiu, J.T. Glessner, K.A. Thomas, E.C. Frackelton, R.M. Chiavacci, M. Imielinski, D.S. Monos, R. Pandey, M. Bakay, S.F.A. Grant, C. Polychronakos, H. Hakonarson, A genome-wide meta-analysis of six type 1 diabetes cohorts identifies multiple associated loci, PLoS Genet. 7 (2011) 1002293, https://doi.org/10.1371/journal.pgen.1002293.